Science Translational Medicine AAAS

Characterization of Circulating Endothelial Cells in Acute Myocardial Infarction

Samir Damani, *et al.*

Sci Transl Med **4**, 126ra33 (2012);
DOI: 10.1126/scitranslmed.3003451

Editor's Summary

Tell-Tale Cells

In Edgar Allan Poe's short story *The Tell-Tale Heart*, the narrator murders an old man and hides the body under the floorboards. The guilty murderer imagines that he hears the beating of the dead man's heart emanating from the corpse underfoot––unwanted evidence of his guilt. But what if the body could leak evidence of a fragile condition before suffering a heart attack? The tale told could be frightening, yes, but the information may allow intervention at a crucial time in the pathophysiological process of heart disease. Now, Damani *et al*. take crucial first steps toward defining a clinical measure that could predict a thus-far unpredictable, myocardial infarction (MI) –associated event: acute atherosclerotic plaque rupture.

Many people tell a personal story of a friend or relative who had a normal stress test just weeks before suffering a heart attack as a result of plaque rupture. Indeed, diagnosis of stable coronary artery disease (CAD) is now possible using stress tests and coronary artery imaging. In contrast, there are no clinically useful tests that warn of impending cardiovascular maladies caused by atherosclerotic plaque rupture. Physicians thus require a noninvasive, clinically feasible assay for a macromolecule or cell in blood that can identify people at risk for this condition, which is increasing in incidence as the population ages and widens. Endothelial cells (ECs) are normally found lining the blood vessels, and leakage into the circulation is evidence of ongoing injury to arteries that occurs on the way to potentially lethal plaque rupture. Elevated amounts of circulating endothelial cells (CECs) were previously linked to acute arterial catastrophes, but these measures have not yet made it into the clinic.

Using automated, clinically feasible, three-channel fluorescence microscopy technology that can detect and permit isolation of rare cells, the authors measured and characterized CECs in healthy subjects and in patients who had experienced a type of heart attack known to manifest after acute arterial plaque rupture. CECs were elevated significantly in patients, relative to controls, and this elevation was not correlated with other measures of heart tissue death. Damani *et al*. also found that acute MI patients specifically displayed multicellular, multinuclear EC clusters and ECs with larger cellular and nuclear areas, relative to age-matched controls and patients with peripheral vascular disease (narrowing of arteries in the legs and feet). Although the study must be conducted in more patients and validated in an independent cohort, the new work suggests that tell-tale CECs may be useful in the clinic as evidence of ongoing plaque rupture and as a warning of possible heart attack in the near future.

Downloaded from stm.sciencemag.org on March 21, 2012

A complete electronic version of this article and other services, including high-resolution figures, can be found at:
http://stm.sciencemag.org/content/4/126/126ra33.full.html

Supplementary Material can be found in the online version of this article at:
http://stm.sciencemag.org/content/suppl/2012/03/19/4.126.126ra33.DC1.html

Information about obtaining **reprints** of this article or about obtaining **permission to reproduce this article** in whole or in part can be found at:
http://www.sciencemag.org/about/permissions.dtl

Science Translational Medicine (print ISSN 1946-6234; online ISSN 1946-6242) is published weekly, except the last week in December, by the American Association for the Advancement of Science, 1200 New York Avenue NW, Washington, DC 20005. Copyright 2012 by the American Association for the Advancement of Science; all rights reserved. The title *Science Translational Medicine* is a registered trademark of AAAS.

PREDICTIVE MEDICINE

Characterization of Circulating Endothelial Cells in Acute Myocardial Infarction

Samir Damani,[1] Andrea Bacconi,[2] Ondrej Libiger,[1,2] Aparajita H. Chourasia,[3] Rod Serry,[4] Raghava Gollapudi,[5] Ron Goldberg,[5] Kevin Rapeport,[5] Sharon Haaser,[1] Sarah Topol,[1] Sharen Knowlton,[1] Kelly Bethel,[2] Peter Kuhn,[2] Malcolm Wood,[2] Bridget Carragher,[2] Nicholas J. Schork,[1,2] John Jiang,[3] Chandra Rao,[3] Mark Connelly,[3] Velia M. Fowler,[2] Eric J. Topol[1,2]*

Acute myocardial infarction (MI), which involves the rupture of existing atheromatous plaque, remains highly unpredictable despite recent advances in the diagnosis and treatment of coronary artery disease. Accordingly, a clinical measurement that can predict an impending MI is desperately needed. Here, we characterize circulating endothelial cells (CECs) using an automated and clinically feasible CEC three-channel fluorescence microscopy assay in 50 consecutive patients with ST-segment elevation MI and 44 consecutive healthy controls. CEC counts were significantly elevated in MI cases versus controls, with median numbers of 19 and 4 cells/ml, respectively ($P = 1.1 \times 10^{-10}$). A receiver-operating characteristic (ROC) curve analysis demonstrated an area under the ROC curve of 0.95, suggesting near-dichotomization of MI cases versus controls. We observed no correlation between CECs and typical markers of myocardial necrosis ($\rho = 0.02$, creatine kinase–myocardial band; $\rho = -0.03$, troponin). Morphological analysis of the microscopy images of CECs revealed a 2.5-fold increase ($P < 0.0001$) in cellular area and a twofold increase ($P < 0.0001$) in nuclear area of MI CECs versus healthy controls, age-matched CECs, as well as CECs obtained from patients with preexisting peripheral vascular disease. The distribution of CEC images that contained from 2 to 10 nuclei demonstrates that MI patients were the only subject group to contain more than 3 nuclei per image, indicating that multicellular and multinuclear clusters are specific for acute MI. These data indicate that CEC counts may serve as a promising clinical measure for the prediction of atherosclerotic plaque rupture events.

INTRODUCTION

Acute myocardial infarction (MI) and ischemic stroke remain leading causes of death and disability worldwide. Each year, more than 2.5 million individuals in the United States alone experience a new or recurrent heart attack or ischemic stroke (*1*). Currently, stable coronary artery disease (CAD) is readily diagnosed through functional stress testing and coronary angiography, whereas cardiovascular events such as MI and ischemic stroke involve atherosclerotic plaque rupture and remain highly unpredictable. To exemplify this point, it is not at all unusual for an individual to have a normal stress test and days to weeks later develop a heart attack or die suddenly, with autopsy evidence of coronary artery plaque rupture as the proximate cause. In addition, previous studies have shown that up to 50% of individuals with MI lack the traditional risk factors for CAD, such as hypertension, elevated low-density lipoprotein (LDL) cholesterol, cigarette smoking, and diabetes (*1*–*5*). Accordingly, a critical need exists for a noninvasive assay for a protein, nucleic acid, or cell type in blood that can identify those individuals who are at the greatest risk for acute arterial disruptive events before they are clinically manifested.

Although the presence of elevated amounts of circulating endothelial cells (CECs) has been associated with acute coronary syndromes, the enumeration of CECs has not been incorporated into clinical practice (*6*–*8*). The principal reasons for this omission include the lack of a practical or widely accepted methodology for quantifying CECs, disparate definitions in the literature for defining CECs, and a lack of in-depth scrutiny of these rare cells when isolated (*9*).

Here, we address these deficiencies using the Veridex CellSearch System, a commercially available rare cell isolation platform, to characterize both the quantitative and the qualitative features of CECs in patients with the highly restrictive MI phenotype; this represents the classic, large heart attack pattern identified by the electrocardiogram known as ST-segment elevation MI (STEMI), which occurs secondary to acute arterial plaque rupture. Further, we sought to determine whether a population of cells isolated from patients with acute MI might show distinctive morphological, antigenic, and genetic signatures that are diagnostic for acute plaque rupture events.

RESULTS

CEC levels are diagnostic of arterial injury in acute MI

The median age for the STEMI patients was 58.5 years (range, 39 to 80 years), with median cardiac troponin and creatine kinase–myocardial band (CK-MB) values—measures of an MI—of 5.7 and 27.9 ng/ml, respectively. Quartiles and ranges for cardiac troponins and CK-MB values in all STEMI cases are shown in Table 1. Notably, the STEMI cases had CK-MB and troponin levels that were, on average, logarithmically higher than clinically accepted normal values (troponin <0.1 ng/ml; CK-MB <3.0 ng/ml) and were well within the range expected for STEMI cases. These values underscore the substantial myocardial necrosis that typically accompanies the STEMI phenotype.

[1]Scripps Translational Science Institute, La Jolla, CA 92037, USA. [2]The Scripps Research Institute, La Jolla, CA 92037, USA. [3]Veridex, LLC, Huntingdon Valley, PA 19006, USA. [4]Palomar Pomerado Health, Escondido, CA 92025, USA. [5]Sharp Memorial and Grossmont Hospitals, San Diego, CA 92123, USA.
*To whom correspondence should be addressed. E-mail: etopol@scripps.edu

Downloaded from stm.sciencemag.org on March 21, 2012

Our strategy to isolate enriched populations of CECs from blood was to use immunomagnetic beads coated with CD146, a cell surface EC glycoprotein, followed by immunostaining and imaging of individual cells by fluorescence microscopy (*10*). Immunomagnetic enrichment using CD146 is an established method used for the enrichment of mature CECs from whole blood (*9*). To ensure that our cellular events were mature ECs, we applied three additional criteria: positive staining for nuclei to eliminate counting of noncellular endothelial microparticles, positive staining for CD105 (an EC marker), and negative staining for CD45 (a leukocyte marker) (fig. S1, A and B). Fifty consecutive STEMI patients (82% male) were prospectively enrolled for cell enumeration. The median CEC ($CD146^+/CD105^+/CD45^-$) count in STEMI patients was 19 cells/ml, with upper and lower quartiles of 12 and 51 cells/ml (range, 2.5 to 465 CECs/ml), respectively (Table 1 and Fig. 1). No correlation was observed between cell counts and initial intramyocardial enzyme concentrations [$\rho = 0.02$, CK-MB; $\rho = -0.03$, troponin (Spearman rank correlation)] (Fig. 2).

Next, CEC enumeration was performed on blood samples from 44 consecutive, healthy controls. The median age of the healthy controls was 30 years (range, 22 to 34 years). The median number of CECs/ml was 3.8 CECs/ml (range, 0.75 to 16.75 CECs/ml), with upper and lower quartile thresholds being 2.25 and 5.06, respectively (Table 1 and Fig. 1). The first 24 healthy controls enrolled in the study were brought back for a repeat measurement 2 months later (Fig. 3), and the median numbers of CECs/ml were unchanged between the first and the second visits, with median values being 3.4 and 3.25 during the first and second visits, respectively ($P = 0.5$, Wilcoxon signed-rank test). These data suggest that CEC levels remain stable over time in healthy individuals. Further, there was no correlation between CEC numbers and age ($\rho = -0.12$).

The observed CEC counts were markedly elevated in our STEMI population when compared to healthy controls [Fig. 1; $P = 1.1 \times 10^{-10}$, Wilcoxon rank-sum test with continuity correction (one-sided)]. A receiver-operating characteristic (ROC) curve associated with a classifier based on logistic regression demonstrated an area under the ROC curve (AUC) of 0.95 (an AUC equal to 1 suggests perfect classification; an AUC equal to 0.5 indicates random selection) (Fig. 1B). This classifier was able to correctly classify 86 (91.5%) of the 94 instances (that is, CEC/ml counts for 50 patients with STEMI and 44 healthy controls) as either an MI case or a healthy control with 10-fold cross-validation. In a 10-fold cross-validation, the data set is partitioned into 10 equally sized subsets. Data from nine subsets are pooled and used to train the classifier, whereas the remaining 10th subset is used as validation data to test the classifier. This process is repeated 10 times. For illustration, a value of 16.5 CECs/ml had a sensitivity (that is, true MI cases classified as such) of 60%, but 98% specificity (that is, true controls classified

Table 1. Phenotypical characteristics of STEMI and control patients. Median values are listed for CECs, troponin, and CK-MB. Quartile values are listed in parenthesis. Normal intramyocardial enzyme levels were <0.1 and <3 ng/ml for troponin and CK-MB, respectively.

Subjects	*n*	Age (range) (years)	% Male	CECs/ml (high, low)	Troponin (ng/ml) (high, low)	CK-MB (ng/ml) (high, low)
STEMI	50	58.5 (39–80)	82	19.4 (11.6, 51.1)	5.2 (1.7, 17.8)	26.9 (8.4, 81.9)
Controls	44	30 (22–34)	51	3.8 (2.3, 5.1)	—	—

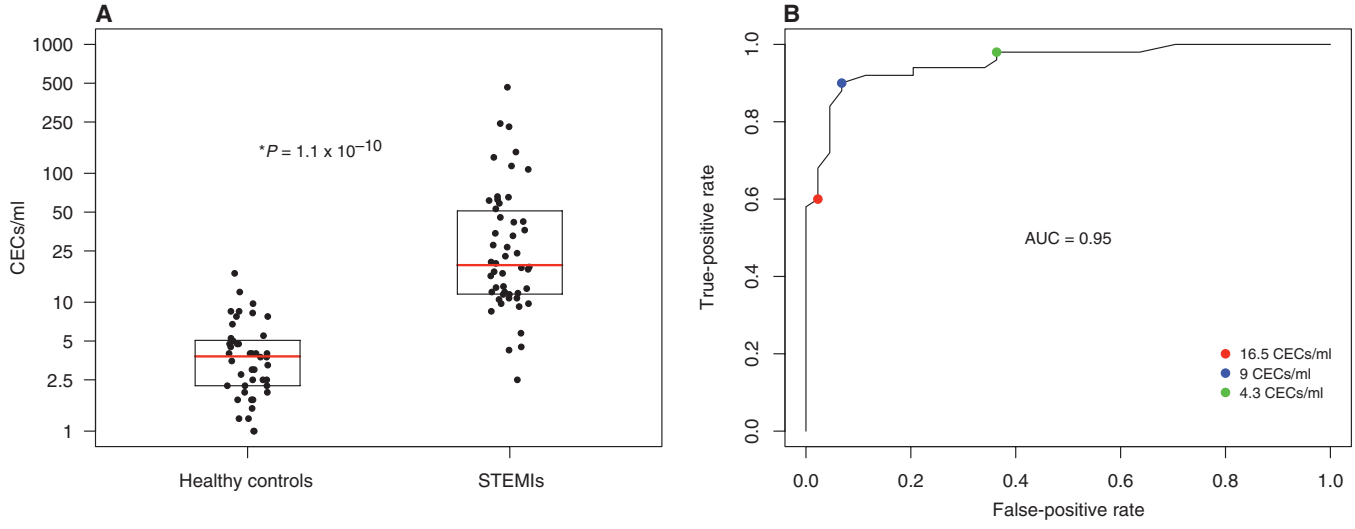

Fig. 1. Enumeration of CECs in healthy controls and STEMI patients. (**A**) CEC quantification in 44 consecutive healthy control and 50 STEMI patients. The median number of CECs in healthy controls was 4 CECs/ml, with upper and lower quartiles of 2 and 5 CECs/ml, respectively. The median number of CECs in STEMI patients was 19 CECs/ml, with upper and lower quartiles of 12 and 51 CECs/ml ($P = 1.1 \times 10^{-10}$, Wilcoxon signed-rank test), respectively. (**B**) AUC was equal to 0.95. The red point represents a classification threshold of 16.5 CECs/ml, which is associated with a sensitivity of 60% and specificity of 98%; blue equals a classification threshold of 9 CECs/ml, with an associated sensitivity of 90% and specificity of 93%; and green equals a threshold of 4.3 CECs/ml, with a 98% sensitivity and 64% specificity for correctly classifying an MI case or control.

Downloaded from stm.sciencemag.org on March 21, 2012

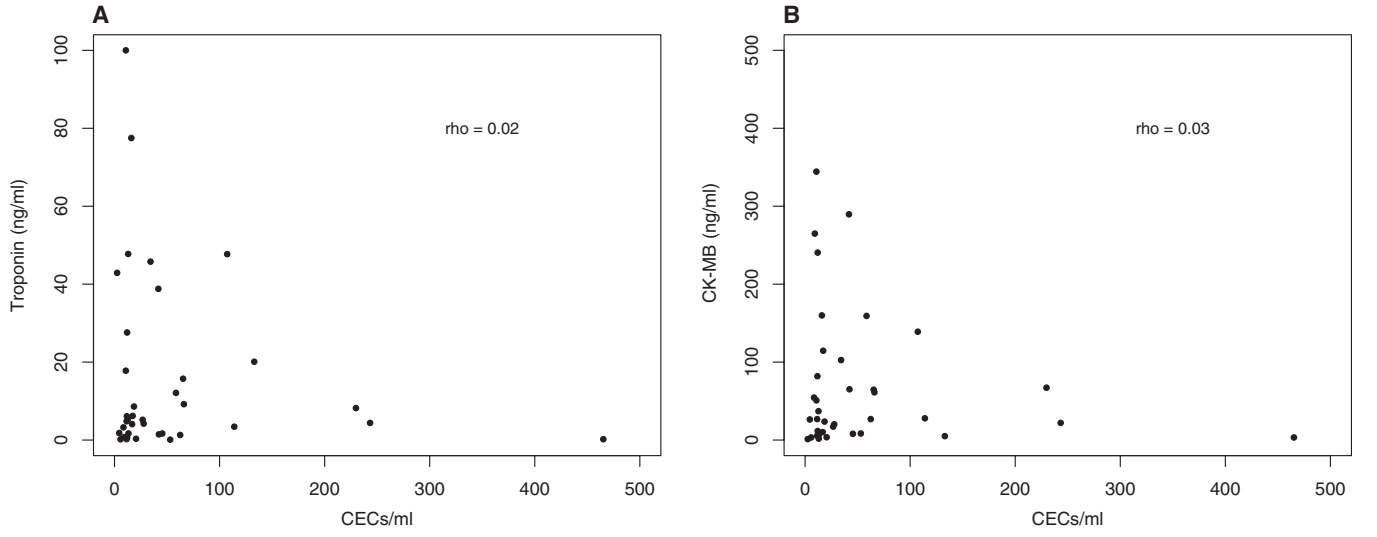

Fig. 2. Correlation between CEC counts and typical markers of myocardial necrosis. (**A**) Using a Spearman rank correlation (rho) coefficient, we assessed CEC counts in MI patients for correlation to initial presenting serum cardiac troponin values. No evidence of correlation was seen (ρ = 0.02, *P* = 0.9). (**B**) No correlation was observed between CEC counts and initial presenting serum CK-MB values (ρ = 0.03, *P* = 0.9).

as such) in the diagnosis of STEMI (Fig. 1B). Alternatively, at a classification threshold of 9 CECs/ml, the associated sensitivity was 90%, whereas the specificity was reduced slightly to 93%. In summary, CEC counts appear to be independent indicators of arterial injury in individuals with acute MI.

CECs from MI patients are abnormally large, misshapen, and may have multiple nuclei

In an attempt to further characterize CECs, we performed a detailed analysis of fluorescent images of isolated CECs from 8 STEMI cases and 10 healthy controls, with the anticipation that a morphological signature of CECs could have incremental diagnostic value compared to the assessment of CEC counts alone. STEMI cases and healthy controls with CEC numbers in the low, middle, and high ranges were selected for analysis (table S1). Additional control populations were also included for this portion of the study, so that any conclusions derived from the morphological appearance of STEMI CECs could be placed in the context of real-world clinical populations. Specifically, 10 consecutive population controls that were age-matched to our STEMI patient group were selected. In addition, two patients with documented peripheral arterial disease who had recently undergone an open vascular procedure were included as a vascular disease control group. Two patients with non–ST-segment elevation MI (NSTEMI) were also included to assess any gross differences in CEC morphology that might distinguish the two MI phenotypes (STEMI versus NSTEMI).

Visual inspection of individual fluorescent CEC images revealed that the morphologies of CECs isolated from MI patients were markedly different from those of controls. Figure 4 illustrates individual CECs isolated from healthy and age-matched controls compared to CECs isolated from a representative STEMI patient (CEC03040). CECs from controls were relatively small, tended to be elongated in shape, and occasionally had two nuclei associated with one cell body, which may represent a cluster of two attached cells or one cell with two nuclei (Fig. 4A, asterisks). In contrast, CECs from STEMI patients were more heterogeneous in appearance, relative to controls, with many cells that were obviously larger than normal and grossly misshapen (Fig. 4B). The nuclei of CECs from the STEMI patient also tended to be larger and aberrantly shaped compared to nuclei of CECs from control individuals (Fig. 4B; also see Fig. 5D). Many of the largest CEC images from

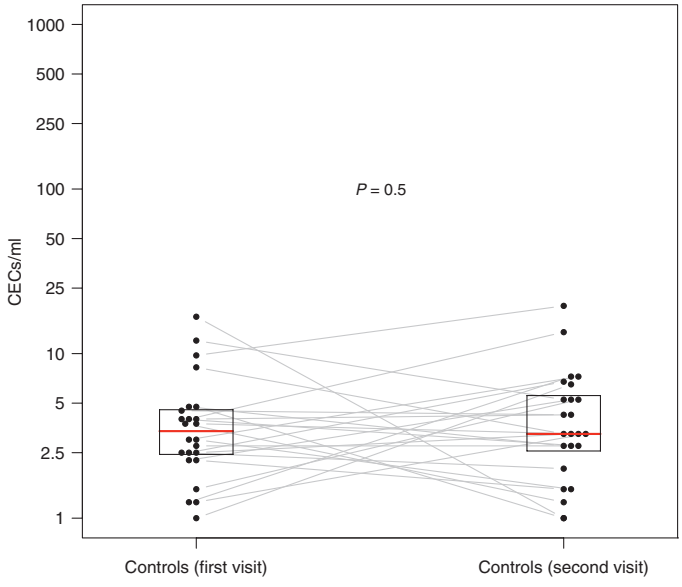

Fig. 3. Stability of CEC counts over time. Two repeat CEC measurements were made in 25 consecutive control individuals at visits separated by a 2-month time frame. Measurements performed on the same individual are connected with a gray line. The CEC counts measured at first visit ranged from 1 to 16.75 CECs/ml, with a median value of 3.38 CECs/ml. On the second visit, the CEC counts measured in the same 24 individuals ranged from 1 to 19.5 CECs/ml, with a median value equal to 3.25 CECs/ml. Using a paired Wilcoxon signed-rank test, we found no evidence of a difference between the CEC counts at the two time points.

Downloaded from stm.sciencemag.org on March 21, 2012

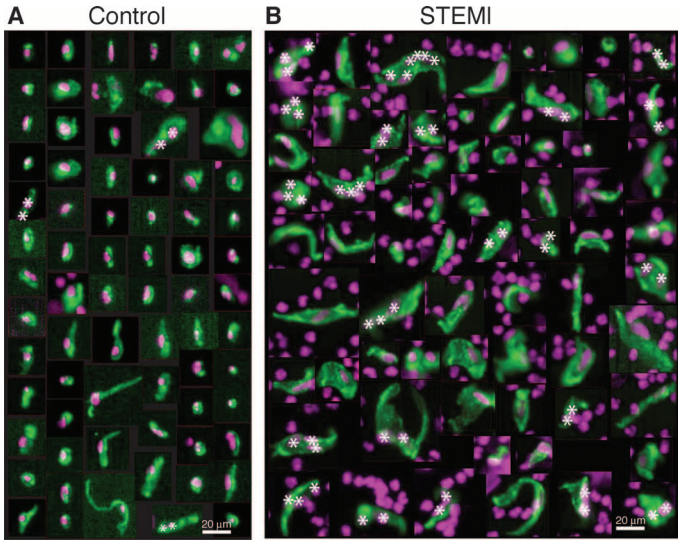

Fig. 4. Fluorescence microscopy images of individual CECs. (**A** and **B**) CECs that were isolated from (A) age-matched controls and (B) a representative STEMI patient (CEC03040). The CECs were labeled with CD105 (green) and DAPI (purple) as markers for their cellular and nuclear compartments, respectively. CECs were identified in these images on the basis of colocalization of CD105 and DAPI staining, resulting in a green cell body overlaying a purple nucleus. Purple nuclei not colocalized with green CD105 staining were contaminating white blood cells also present in the field of view (on the basis of positive staining for CD45). CECs from the STEMI patient were heterogeneous in size and shape, and many of them were much larger than CECs from control subjects and appeared to have multiple nuclei. Image magnification is constant for all images. All CEC images from three age-matched control individuals are shown, and 69 CEC images were randomly selected for presentation from STEMI patient CEC03040, who had blood of 58 CECs/ml, which was in the mid range of CECs/ml for the MI patients in this study. Scale bars, 20 μm. Asterisks, multiple nuclei associated with one CD105-stained cell body.

STEMI patients often contained several nuclei associated with one continuous CD105-stained cell body region, thus appearing as multinuclear clusters with up to 10 nuclei per cluster (Fig. 4B; also see below, Fig. 6). Because cell-cell boundaries were not clearly demarcated in these fluorescence images, it is not possible to determine rigorously whether these are multicellular clusters or, alternatively, multinuclear individual cells.

To substantiate the qualitative differences apparent by visual inspection of CEC images from control and MI patients (Fig. 4), we developed a custom image analysis software method to measure cellular and nuclear areas for individual images of CECs (fig. S1C). CEC morphologies in 50 to 100 randomly selected images were analyzed for each MI patient and compared to all CEC images from control patients. This analysis revealed that the mean cellular area of CECs from MI patients was ~270 μm^2, more than 2.5-fold greater than the mean ~100-μm^2 cellular area of CECs from either healthy or age-matched controls ($P < 0.0001$, Student's t test) (Fig. 5A). Similarly, the mean area of CEC nuclei from MI patients was ~65 μm^2, significantly larger than the 30- to 40-μm^2 area for CEC nuclei from healthy or from age-matched controls ($P < 0.0001$, Student's t test) (Fig. 5B). In contrast, the morphological parameters for CECs from patients who were about to undergo vascular surgery for non–cardiac-related conditions were not significantly different from that of controls (Fig. 5, A and B) [Fig. 5A: $P = 0.38$ and $P = 0.03$ for vascular versus healthy and vascular versus age-matched controls, respectively; Fig. 5B: $P = 0.48$ or $P = 0.28$ for vascular versus healthy and vascular versus age-matched controls, respectively (based on Student's t tests)]. Finally, the ratio of the cellular/nuclear area was ~1.5 fold greater for CECs from MI patients compared to CECs from any of the control groups, with a significance level of $P < 0.0001$ for healthy or age-matched versus MI patients, and $P = 0.002$ for vascular versus MI patients (Student's t test). Representative examples of the ranges of cellular and nuclear size variations for CEC images of single cells from control subjects and MI patients analyzed are shown in Fig. 5D.

Although the cellular and nuclear areas of CECs from age-matched controls tended to be somewhat larger than those of CECs from healthy, younger controls (Fig. 5, A and B), the cellular/nuclear area ratios were not different between these two control groups ($P = 0.49$, Student's t test) (Fig. 5C). This observation indicates that the cellular and nuclear areas increased proportionately for CECs from age-matched compared to healthy controls, whereas the cellular area increased disproportionately to the nuclear area for CECs from MI patients. Therefore, the increased cellular/nuclear area ratio is a morphological abnormality specific to MI patients, because it was not observed for either age-matched or vascular control patients in comparison to healthy young controls. In conclusion, our qualitative visual observations (Fig. 4) and our quantitative image analysis (Fig. 5) demonstrated that, compared to controls, CECs from MI patients were significantly larger, with larger mean cell sizes and nuclei and a greater ratio of cellular to nuclear area. A comparison between the STEMI and the NSTEMI CECs analyzed for the cellular and nuclear areas as well as the cellular/nuclear area ratios did not show any significant differences between the two groups (fig. S2).

Next, we analyzed the images to determine the percent of CECs present as single cells with one nucleus or as cells with two or more nuclei, for CECs from both MI patients and controls. Examples of individual CEC images with multiple nuclei (from MI patients) are illustrated in Fig. 6A. Quantitative analysis revealed that, on average, ~25% of the CEC images from MI patients contained two or more nuclei, compared to 5 to 10% of CEC images from the healthy or age-matched controls, which is a severalfold increase in the numbers of nuclei per image ($P = 0.0008$, Student's t test) (Fig. 6B). Although the percent of CEC images with multiple nuclei also appeared to be increased in the age-matched control group with respect to the healthy control or vascular group, this difference was not statistically significant because of the variability in this parameter in these two groups ($P = 0.23$, Student's t test) (Fig. 6B). The distribution of CEC images that contained from 2 to 10 nuclei demonstrated that MI patients are the only group in this study to contain more than 3 nuclei per image (Fig. 6C). In contrast, most of the CEC images from healthy, age-matched controls or vascular patients contained only one or two nuclei (Fig. 6C). Ten percent to 15% of CEC images for both control and MI patients contained two nuclei, which may represent individual binuclear cells (a characteristic feature of mature endothelium). However, inspection of individual CEC images from MI patients with multiple (more than two) nuclei revealed a multilobular morphology in many cases, suggesting that at least some of these images result from groups of several CECs attached to one another. A previous study also observed images

Downloaded from stm.sciencemag.org on March 21, 2012

of CECs isolated from MI patients showing multiple nuclei, which could constitute multicellular clusters (*8*). In summary, we conclude that CECs from MI patients exhibit distinctive and quantifiable morphological features (increased size and multinuclearity parameters), which can provide additional indicators of arterial injury in individuals with acute MI.

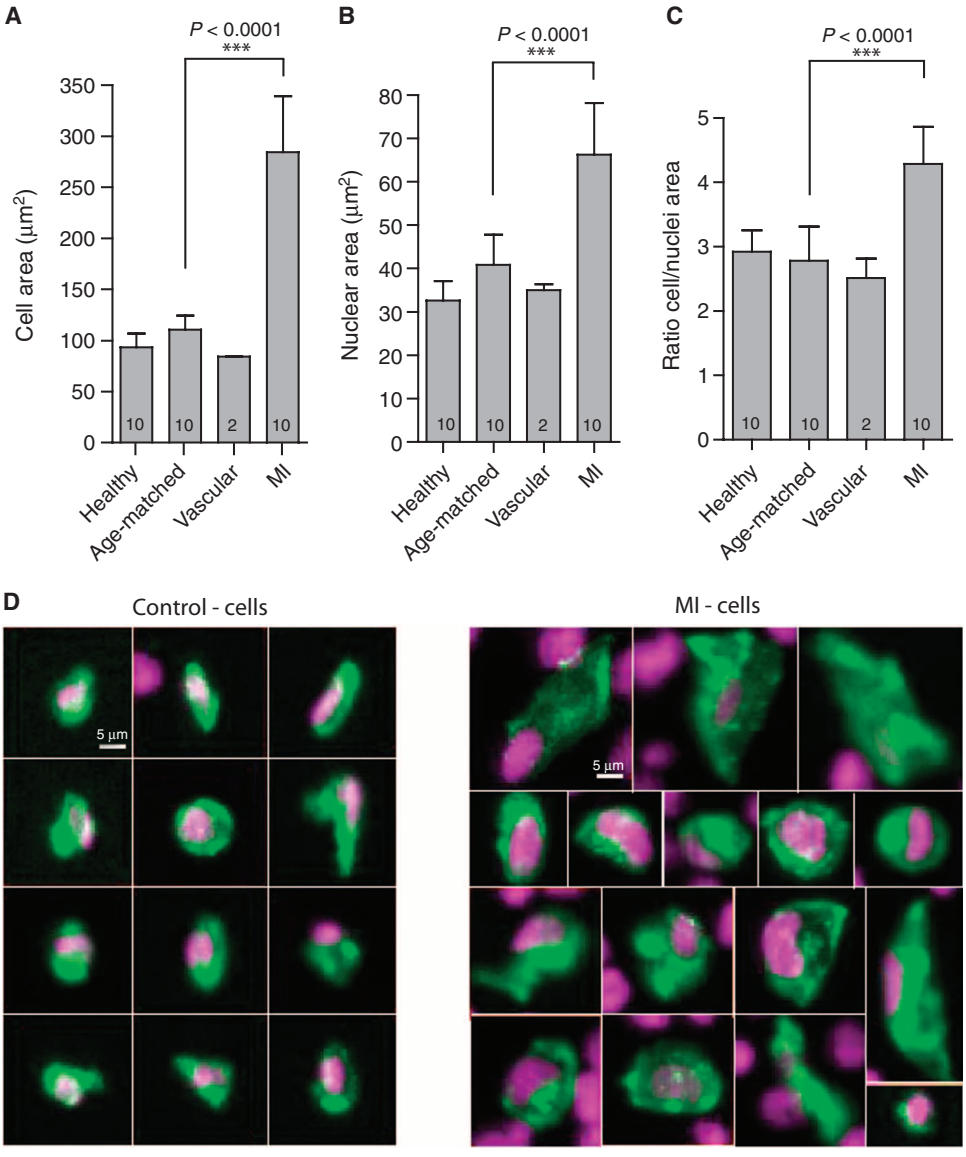

Fig. 5. CEC size analysis for age-matched and healthy control subjects, vascular control subjects, and MI (STEMI and NSTEMI) patients. (**A**) Cellular areas (μm^2) for cells from each group (mean ± SD). *P* values: 0.0133 (healthy versus age-matched); 0.3786 (healthy versus vascular); 0.0286 (age-matched versus vascular); <0.0001 (healthy versus MI); <0.0001 (age-matched versus MI); 0.003 (vascular versus MI), based on Student's *t* tests. (**B**) Nuclear areas (μm^2) for cells from each group (mean ± SD). *P* values: 0.007 (healthy versus age-matched); 0.482 (healthy versus vascular); 0.282 (age-matched versus vascular); <0.0001 (healthy versus MI); <0.0001 (aged-matched versus MI); 0.0059 (vascular versus MI), based on Student's *t* tests. (**C**) Ratios between the cellular area and the nuclear area for cells from each patient group (mean ± SD). *P* values: 0.4848 (healthy versus age-matched); 0.14 (healthy versus vascular); 0.53 (age-matched versus vascular); <0.0001 (healthy versus MI); <0.0001 (age-matched versus MI); 0.0021 (vascular versus MI), based on Student's *t* tests. Numbers in each bar for (A) to (C) represent the number of patients analyzed from each group; all CECs from each control individual and 50 to 100 CECs randomly selected from each MI patient were analyzed. Image magnification was constant for all images. (**D**) Representative images of CECs from control (age-matched and healthy) and MI (STEMI and NSTEMI) patients, illustrating typical CECs (that is, mean area sizes) and the ranges of variations in CEC area sizes from these groups. CECs were identified with CD105 (green) and DAPI (purple) staining as markers for cellular and nuclear compartments, respectively. Scale bars, 5 μm.

DISCUSSION

The lack of normal endothelial integrity is thought to be the unifying principle for susceptibility to atherosclerotic plaque rupture as well as other arterial, nonatherosclerotic vessel wall rupture or fissure events (*11*–*13*). Recent autopsy data demonstrating the presence of multiple healed nonlethal plaque ruptures in the coronary arteries of sudden cardiac death victims suggest that ongoing arterial injury is actively transpiring during the time leading up to an acute arterial catastrophe (*14*, *15*). Accordingly, the proposed framework of EC disruption from plaque rupture sites and their detection in the peripheral circulation in patients with MI and stroke is based on well-established biological principles. Here, we have demonstrated the ability to identify, enumerate, and quantitatively characterize the morphology of CECs from patients with acute MI using an automated rare cell imaging system in combination with fluorescence image computational analysis. Our method is tantamount to a fluid-phase biopsy of the coronary artery that would otherwise be impossible to obtain in a living person and, therefore, provides a unique window into the disease from the precise cells that are being shed as a result of injury to inflamed arterial segments.

The main advance of this work is the identification of distinct morphological characteristics of CECs from patients with an MI event. This was made possible by the use of a validated and automated technology in the form of a three-channel fluorescence assay. The dysmorphic features of the CECs from individuals with MI, which have not been previously described, provide support that abnormal endothelial biology is likely a critical contributor to acute plaque rupture events, which is pathognomonic for heart attack and ischemic stroke.

To date, reports of CEC levels have varied greatly in the published literature. This variability stems primarily from the use of highly divergent CEC isolation methods and variable immunophenotypical definitions of CECs (*9*, *16*). To overcome these

Downloaded from stm.sciencemag.org on March 21, 2012

deficiencies, we have used the CellTracks image analyzer system for this study, which is the only CEC isolation methodology that has been validated by a protocol using the National Committee for Clinical Laboratory Standards guidelines (*10*). The CD146 enrichment step followed by the multimarker identification strategy of positive and negative selection criteria that we used minimizes the analytical variability that frequently accompanies the processing of large sample volumes. Moreover, the use of validated, standardized criteria for signal intensity and automated image analysis allows for better reproducibility of results by reducing the interoperator variability (*10*). Finally, all blood was collected from acute MI cases before diagnostic angiography and angioplasty, thus preventing contamination of MI-derived CECs with cells released from the arterial endothelium as a result of mechanical disruption by catheters and coronary stents used in the treatment of coronary artery obstructions. This fact and the sole inclusion of patients with STEMI—a phenotype that denotes an underlying acute arterial plaque rupture—lends further support to the notion that CECs present in patients with acute MI are cells that have been sloughed from injured arterial segments.

Our study shows that median CEC counts in MI patients are more than 400% higher than in those found in healthy controls. Moreover, we have also demonstrated that CEC levels tend to remain stable over time in healthy individuals. On its own, the ROC curve analysis demonstrates that CEC counts provide an accurate means for classifying individuals as a case or control. Particularly noteworthy was the absolute lack of correlation between CEC counts and typical markers of ischemia in our MI population and the lack of correlation between CEC counts and age in our controls. Together, these findings bolster existing data that suggest that elevated levels of CECs are independent predictive indicators of arterial injury in a variety of atherothrombotic conditions including unstable angina (a precursor syndrome to MI, typically leading to MI within 1 to 2 weeks if left untreated), NSTEMI, and ischemic stroke (*6*–*8*). This is an especially important point, because the objective of this work is to identify a means of tagging an active plaque rupture event before myocardial necrosis has ensued. There are very refined methods for detecting myocardial necrosis with ultrasensitive troponins, and excellent means of diagnosing stable obstructive coronary atherosclerotic plaque via stress testing and coronary angiography. But to date, a clinical predictor of imminent plaque rupture has not been identified.

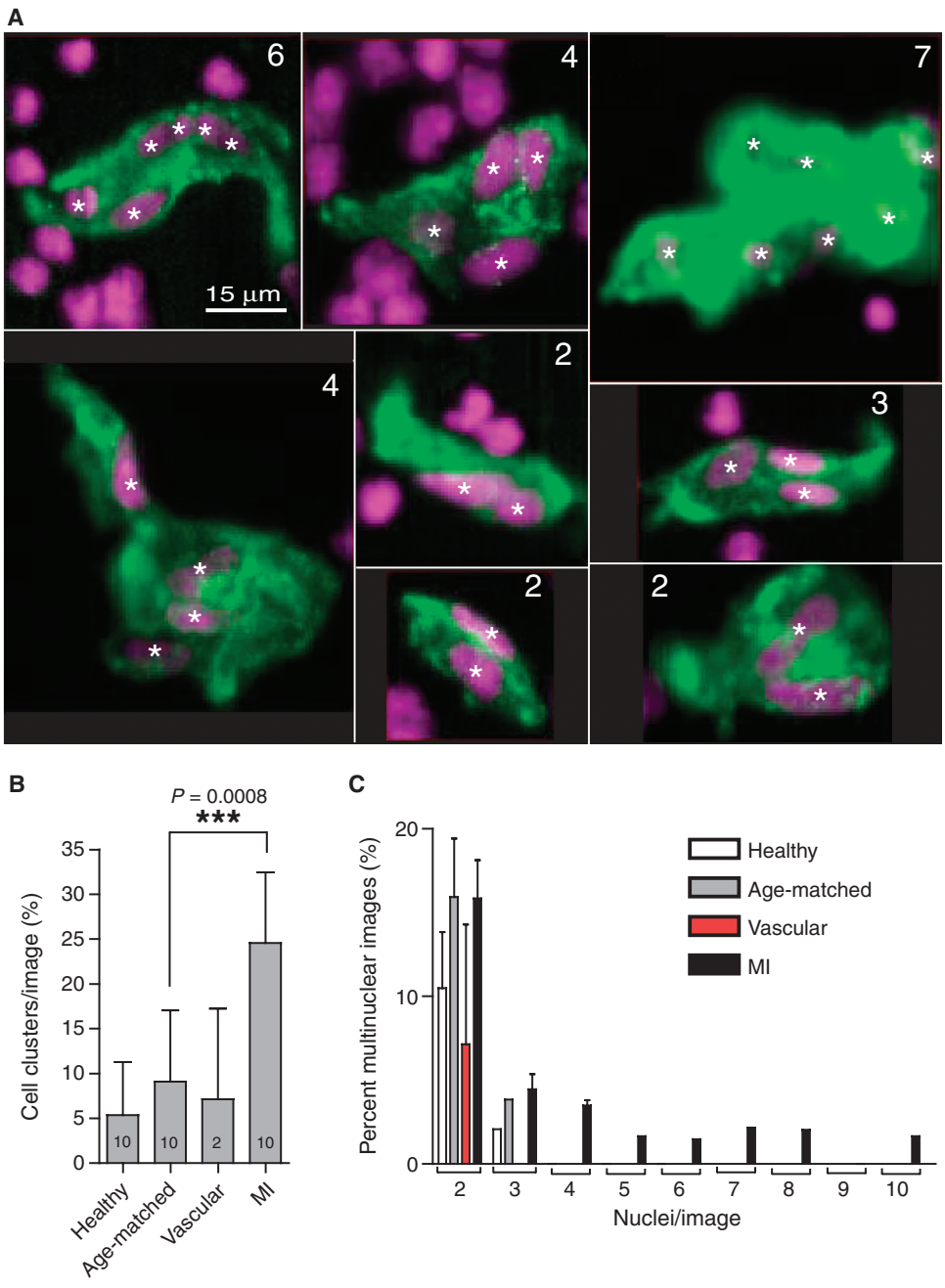

Fig. 6. Analysis of numbers of CECs with multiple nuclei from control subjects, random age-matched control subjects, vascular control subjects, and MI (STEMI and NSTEMI) patients. (**A**) Images of CECs with multiple nuclei from the STEMI patient group stained with CD105 (green) and DAPI (purple, white asterisks) to identify the cellular and the nuclear compartments, respectively. The number of nuclei per CD105-stained cell body is specified in the upper right of each image. Image magnification was constant for all images. Scale bar, 15 μm. (**B**) Percent of CEC images with multiple nuclei (two or more nuclei per image) in each group (mean ± SD). The numbers in each bar represent the number of individuals analyzed. (**C**) Distribution of the numbers of nuclei per image for the various subject groups (mean ± SD). Bars indicate healthy (white) and age-matched (gray) controls, vascular controls (red), and MI (black) patients. *P* values: 0.2295 (healthy versus age-matched); 0.0008 (age-matched versus MI); 0.0231 (vascular versus MI), based on Student's *t* tests.

Downloaded from stm.sciencemag.org on March 21, 2012

Beyond simple CEC count data, we observed that MI CECs showed a specific set of measurable differences in morphological parameters, namely, cell and nuclear areas, ratio of cellular/nuclear area, and association with multiple nuclei, when compared to various control groups. We took stringent measures to be sure this finding was authentic. First, we developed a customized image analysis Matlab program written specifically for this purpose to quantify and qualify all visual observations, thereby removing any bias that may be introduced by a qualitative or manual assessment of cellular characteristics (fig. S1C). Second, we randomly selected CECs from 10 separate MI cases that included individuals with CEC ranges from low to high numbers to get a global estimate of all pertinent cellular features across the MI patient population (table S1). Third, we obtained additional control populations, because we hypothesized that CEC morphology in healthy young controls might be different from that of a healthy older population or those with existing vascular disease.

Accordingly, we found no significant differences in cellular and nuclear sizes, ratios, or presence of multiple nuclei between any of the various control groups (Figs. 5 and 6, see legends). However, in the age-matched control group only, there was a tendency toward both increased cell and nuclear size and number compared with the healthy (younger) controls. Although this difference did not reach statistical significance, it may be that some individuals with undiagnosed arterial disease or impending cardiac events were included in this older population-based sample. In addition, we found no statistically significant differences between STEMI and NSTEMI CECs. This suggests that individuals with disparate presentations of acute coronary syndromes share similar CEC phenotypes, indicating a common underlying pathological link.

The specific morphological features of CECs from MI patients, including their larger sizes and presence of multiple nuclei, may reflect their site of origin and provide clues to pathological processes that lead to arterial injury and sloughing of the endothelium. A mature endothelial origin for $CD146^+/CD105^+/CD45^-$ cells is presumptive but supported by several lines of evidence presented here, including the capture of these cells using anti-CD146, their expression of CD105, and, moreover, their lack of CD45 expression. This phenotype can be shared by bone marrow–derived mesenchymal cells; however, the lack of CD45 expression positivity makes it unlikely that the cells we counted as CECs were activated T cells and mesenchymal hematopoietic precursors. In addition, we show that the $CD146^+/CD105^+/CD45^-$ cells captured also expressed CD31 (fig. S3A), a marker found on vascular endothelium but not on bone marrow–derived mesenchymal cells. The morphology of CECs was also inconsistent with the scant cytoplasm, spindle shape, and smaller size typical of mesenchymal and endothelial progenitor cells. Gene expression analysis of CEC-enriched cells (fig. S4, A and B) showed elevation of the endothelial-specific markers endothelin and von Willebrand factor (vWF) in STEMI patients relative to non-MI controls and peripheral blood mononuclear cells. Finally, CECs were also $CD34^+$ (fig. S3B) and $CD146^+$, consistent with an endothelial origin but not consistent with their being activated T cells, bone marrow–derived mesenchymal cells, or endothelial progenitor cells.

The CECs in MI patients may derive from older, and thus larger, cells in the arterial endothelium, with injured cells released singly or as multicellular groups or sheets from injured regions during plaque rupture. CEC clusters in MI patients may also result from abnormal aggregation of injured cells disturbed during their passage through the circulation. By contrast, the smaller, less clustered (and fewer) CECs in control individuals may reflect infrequent release of younger and thus smaller ECs from regions of remodeling or proliferating vasculature in which ECs might normally lose their attachments. Future immunostaining of CECs from MI patients and controls with markers for endothelial activation and injury, cell junctions, and cell-substrate attachments, as well as cell cycle and signaling pathways, may be helpful to uncover molecular and cellular mechanisms of arterial injury in patients with MI. Our automated strategy for enrichment, immunostaining, fluorescence imaging, and computational analysis of CEC morphology lays the groundwork for more in-depth molecular, cellular, and ultrastructural assessments of CECs in a variety of clinical conditions.

In summary, using an automated cell isolation and imaging platform and blood samples from patients with acute MI, we show that there is a clear excess of CECs and that these cells have discrete antigenic and morphological signatures. These distinctive cell characteristics may be useful in developing a refined biomarker for arterial injury. Systematic application of such CEC biomarkers to prospective studies that assess the predictive potential of CECs in those at high risk for arterial injury syndromes will be needed for further validation. In addition, future studies are necessary to investigate the possible correlation between the altered cellular morphology of MI CECs and a unique genomic signature of these cells. Our findings may ultimately support the development of an assay to help predict imminent risk of a heart attack.

MATERIALS AND METHODS

Patient selection and specimen collection

Between January 2010 and February 2011, patients who presented to the emergency room with STEMI at four regional medical centers in San Diego County had blood drawn for CEC characterization. Patients were enrolled prospectively in consecutive fashion on the basis of appropriate eligibility criteria (below). All STEMI blood samples were obtained in the cardiac catheterization laboratory via an arterial sheath and before catheter insertion for diagnostic coronary angiography or intervention. All patients met criteria for STEMI including ST-segment elevation of at least 0.2 mV in two contiguous precordial leads or 0.1 mV in contiguous limb leads. Positive markers of myocardial ischemia (CK-MB or troponin) and angiographic evidence of obstructive CAD were also required. Initial cardiac troponin and CK-MB values were obtained and recorded. Subsequent CK-MB and troponin values were not recorded.

Healthy controls were recruited from the normal blood donor program at the Scripps Research Institute for the purpose of comparing CEC levels and morphology to such measures obtained from STEMI patients. All healthy controls were between the ages of 18 and 35 and were deemed free of any chronic disorders via self-report. Blood for CEC ascertainment in healthy and random age-matched samples was obtained via venipuncture. Randomly selected samples of age-matched controls, who via self-report denied the presence of any acute illnesses or symptoms, were included in the CEC morphology analysis portion of the study. Smoking status, obesity, family history of cardiovascular disease, or acute febrile illness was not used as exclusionary criteria. Individuals with existing vascular disease who recently underwent an open endarterectomy procedure along with patients with NSTEMI were

Downloaded from stm.sciencemag.org on March 21, 2012

also recruited for the sole purpose of morphological characterization of their CECs. Criteria for MI in the NSTEMI population included symptoms consistent with MI, serological evidence of myocardial necrosis (as determined by elevated amounts of cardiac troponins and CK-MB), and angiographic evidence of obstructive CAD.

All blood from cases and controls was collected in CellSave tubes that contained a mild cellular fixative known to stabilize CEC levels. Subsequently, samples were kept at room temperature and shipped via courier to a central lab for processing within 48 hours of collection. Institutional review board approval was obtained from all recruiting sites, and all patients gave informed consent.

Identification of CECs by CellTracks system

The CellTracks system consists of an automated CellTracks AutoPrep sample preparation device and a CellTracks Analyzer II (CTA II) image analysis platform. The CellTracks system used the CellSearch endothelial cell kit to automate all sample enrichment and staining steps as described previously (*10*). Briefly, CECs in whole blood were bound by anti-CD146 antibody–conjugated magnetic nanoparticles and enriched by repeated magnetic incubations and automated washings. $CD146^+$-enriched cells were stained with 4′,6-diamidino-2-phenylindole (DAPI) for nuclei, and with fluorescent antibodies to CD105 and CD45, and the magnetically enriched and fluorescent-labeled cells were placed into a MagNest Cell Presentation Device. The steps during sample and image analysis by CTA II are shown in fig. S1A. The MagNest device consists of a disposable sample cartridge positioned between two permanent magnets to orient the magnetically labeled cells in a monolayer for fluorescent image analysis. The MagNest is placed in the CTA II, a four-color semiautomated fluorescence microscope. The analyzer then scans the entire cartridge surface, collecting images for each of the four fluorescent colors. It records 180 images for each fluorescent channel (720 images per scan). The CTA II's software automatically analyzes each frame and identifies those objects within the frame that, based on their DAPI and CD105 fluorescence, were possible candidate CECs. The candidate CECs were placed as a series of thumbnails in an image gallery for review and identification by a trained operator (fig. S2A). The thumbnail images show, from right to left, an unused [fluorescein isothiocyanate (FITC)] channel, CD45-APC (allophycocyanin) signal, DAPI-stained nuclei, CD105-PE (phycoerythrin) reactivity, and, finally, an overlay of the CD105-PE and DAPI staining. The FITC channel can be used to phenotype CECs with additional markers of interest. To be scored as a CEC, a cell had to have a nucleus, express CD105, have the morphology of a cell, and be negative for CD45. An example of three objects as presented to the reviewer by the CTA II software is shown in fig. S1B. The first two objects met the criteria and were scored as CECs by the operator (checked box). The third object was judged a leukocyte because it was $CD45^+$ (box not checked). The software automatically tabulated the checked boxes within each sample, and results were expressed as the number of CECs per 4 ml of blood.

$CD146^+/CD105^+/CD45^-$ cells were also reacted with an antibody to CD31 or to CD34 to characterize the cells and better determine their likely origin. The marker CD31-FITC or CD34-FITC was added during sample preparation on the CellTracks AutoPrep system as described above. CD31-FITC and CD34-FITC were purchased from BD Biosciences and used at a final concentration of 1 μg/ml. $CD146^+/CD105^+/CD45^-$ cells that expressed CD31 and CD34 stained positive and appeared in the thumbnail images in the corresponding FITC channel. The $CD31^+$ and $CD34^+$ CECs are shown in fig. S3.

CEC morphology analysis

CEC image analysis was performed with a customized Matlab program (The MathWorks; release 2009b or newer) written for this purpose. Data analysis was performed with either Matlab or GraphPad Prism (release 4.00). Fluorescence intensity measurements of fixed CECs from CellSearch (Veridex) were carried out in a four-step process (fig. S1C): (i) cropping and separation of single CEC color images into their individual channels (CD105 and DAPI), which were then saved as tiff files; (ii) cell body (CD105) and nuclear (DAPI) segmentation; (iii) area calculation of the segmented images; and (iv) single cell and nuclear area calculation. Two Gaussian transformations with SDs of σ1 and σ2 were calculated for the CD105 and DAPI channels of each CEC image. The background pixels were removed with unimodal thresholding (*17*), and the final objects that corresponded to CEC cell bodies and nuclei were determined as thresholded difference of two Gaussians images. The set of SD σ1 and σ2 used in the Gaussian transformations was chosen to generate the most accurate mask by visual inspection. The area of the CD105 channel for each CEC image was divided by the number of nuclei identified in the nuclear masks contained within the CD105 area. Data analysis was performed with either Matlab or GraphPad Prism (release 4.00). All statistical comparisons between two populations were performed with an unpaired Student's *t* test (two-tailed) in GraphPad Prism (release 4.00).

CEC gene expression analysis

Two 10-ml EDTA-containing Vacutainer tubes (Becton Dickinson) were used to collect blood from 12 MI patients and 13 age-matched healthy donors. CECs were isolated with the CellSearch system with the CellSearch CEC Profile kit (Veridex, LLC). A 1-ml aliquot of TRIzol reagent (Life Technologies) was added to the isolated CECs, and the samples were stored at −80°C until use. Total RNAs were isolated from CECs according to the standard TRIzol method provided by the manufacturer. The quantity and quality of RNA were examined with NanoDrop 1000. Total RNA (50 ng) was first converted to labeled target complementary DNA (cDNA) with the Ovation RNA Amplification System V2 (NuGEN). Subsequently, 3.75 μg of the purified cDNA underwent a two-step fragmentation and labeling process with the Encore Biotin Module (NuGEN). Targets were hybridized to Affymetrix human U133 Plus 2.0 arrays according to protocols suggested by the supplier (Affymetrix). After hybridization, arrays were washed and stained with standard Affymetrix procedures before scanning on the Affymetrix GeneChip Scanner and data extraction with Expression Console. Each probe set was considered a separate gene. Expression values for each gene were calculated with the robust multiarray analysis (RMA) method.

Statistical analysis of CEC counts

A two-sample test for the nonparametric Behrens-Fisher problem was used to determine whether STEMI cases exhibited higher counts of CECs compared to controls. Spearman rank correlation was used to determine whether there was a linear relationship between the number of CECs and the amounts of serum CK-MB and cardiac troponin as well as age. We built a mathematical model using logistic regression with 10-fold cross-validation that classified patients into two groups, STEMI and controls, based on their observed CEC counts. This model, generated in Weka software (*18*), was used to assess the number of correctly classified instances and the AUC. The ROC curve shown in Fig. 1B is based on a logistic regression model using all available data (that

Downloaded from stm.sciencemag.org on March 21, 2012

is, without cross-validation) and was generated with the ROCR package of the R statistical computing environment (*19*). The AUC was calculated with the somers2 function of the Hmisc package in the R statistical computing environment (*20*).

Statistical analysis for endothelin and vWF levels

The difference between the numbers of CECs in control and MI groups for both endothelin 1 and vWF was statistically different by both parametric and nonparametric testing. A Student's *t* test was used with the variance of each group treated as unequal. The values in fig. S4, A and B, were scaled to log base 2. On this scale, an increase of one would represent a doubling of the magnitude of the difference between the two means on a natural scale. Note that the difference between these two groups remained significant if we switched to a nonparametric test. The Mann-Whitney test *P* value for endothelin was 5.34×10^{-5} and for vWF was 0.00123. Unlike with the Student's *t* test, a normal distribution is not assumed, and this *P* value would not change as a result of any scaling of the data.

SUPPLEMENTARY MATERIALS

www.sciencetranslationalmedicine.org/cgi/content/full/4/126/126ra33/DC1

Fig. S1. Image analysis by the CellTracks Analyzer II and identification of CECs.

Fig. S2. CEC size analysis for STEMI and NSTEMI patients.

Fig. S3. CellTracks Analyzer II browser images of $CD105^{+}$/ $CD45^{-}$ cells stained with CD31 or CD34 marker.

Fig. S4. Expression of (**A**) ELN1 and (**B**) vWF in 12 myocardial infarction (MI) patients and 13 age-matched healthy donors (Normal).

Table S1. CEC counts in MI cases and controls used for morphologic analysis.

REFERENCES AND NOTES

1. E. Braunwald, Shattuck lecture—Cardiovascular medicine at the turn of the millennium: Triumphs, concerns, and opportunities. *N. Engl. J. Med.* **337**, 1360–1369 (1997).
2. C. H. Hennekens, Increasing burden of cardiovascular disease: Current knowledge and future directions for research on risk factors. *Circulation* **97**, 1095–1102 (1998).
3. R. F. Heller, S. Chinn, H. D. Pedoe, G. Rose, How well can we predict coronary heart disease? Findings in the United Kingdom Heart Disease Prevention Project. *Br. Med. J. (Clin. Res. Ed.)* **288**, 1409–1411 (1984).
4. L. G. Futterman, L. Lemberg, Fifty percent of patients with coronary artery disease do not have any of the conventional risk factors. *Am. J. Crit. Care* **7**, 240–244 (1998).
5. L. Tavazzi, Clinical epidemiology of acute myocardial infarction. *Am. Heart J.* **138**, S48–S54 (1999).
6. C. J. Boos, S. K. Soor, D. Kang, G. Y. Lip, Relationship between circulating endothelial cells and the predicted risk of cardiovascular events in acute coronary syndromes. *Eur. Heart J.* **28**, 1092–1101 (2007).
7. J. Quilici, N. Banzet, P. Paule, J. B. Meynard, M. Mutin, J. L. Bonnet, P. Ambrosi, J. Sampol, F. Dignat-George, Circulating endothelial cell count as a diagnostic marker for non–ST-elevation acute coronary syndromes. *Circulation* **110**, 1586–1591 (2004).
8. M. Mutin, I. Canavy, A. Blann, M. Bory, J. Sampol, F. Dignat-George, Direct evidence of endothelial injury in acute myocardial infarction and unstable angina by demonstration of circulating endothelial cells. *Blood* **93**, 2951–2958 (1999).
9. A. Woywodt, T. Kirsch, M. Haubitz, Immunomagnetic isolation and FACS—Competing techniques for the enumeration of circulating endothelial cells. *Thromb. Haemost.* **96**, 1–2 (2006).
10. J. L. Rowand, G. Martin, G. V. Doyle, M. C. Miller, M. S. Pierce, M. C. Connelly, C. Rao, L. W. Terstappen, Endothelial cells in peripheral blood of healthy subjects and patients with metastatic carcinomas. *Cytometry A* **71**, 105–113 (2007).
11. J. C. Sluimer, F. D. Kolodgie, A. P. Bijnens, K. Maxfield, E. Pacheco, B. Kutys, H. Duimel, P. M. Frederik, V. W. van Hinsbergh, R. Virmani, M. J. Daemen, Thin-walled microvessels in human coronary atherosclerotic plaques show incomplete endothelial junctions relevance of compromised structural integrity for intraplaque microvascular leakage. *J. Am. Coll. Cardiol.* **53**, 1517–1527 (2009).
12. R. Ross, Atherosclerosis—An inflammatory disease. *N. Engl. J. Med.* **340**, 115–126 (1999).
13. R. Ross, The pathogenesis of atherosclerosis: A perspective for the 1990s. *Nature* **362**, 801–809 (1993).
14. M. C. Kramer, S. Z. Rittersma, R. J. de Winter, E. R. Ladich, D. R. Fowler, Y. H. Liang, R. Kutys, N. Carter-Monroe, F. D. Kolodgie, A. C. van der Wal, R. Virmani, Relationship of thrombus healing to underlying plaque morphology in sudden coronary death. *J. Am. Coll. Cardiol.* **55**, 122–132 (2010).
15. A. P. Burke, F. D. Kolodgie, A. Farb, D. K. Weber, G. T. Malcom, J. Smialek, R. Virmani, Healed plaque ruptures and sudden coronary death: Evidence that subclinical rupture has a role in plaque progression. *Circulation* **103**, 934–940 (2001).
16. C. J. Boos, G. Y. Lip, A. D. Blann, Circulating endothelial cells in cardiovascular disease. *J. Am. Coll. Cardiol.* **48**, 1538–1547 (2006).
17. P. L. Rosin, Unimodal thresholding. *Pattern Recognit.* **34**, 2083–2096 (2001).
18. M. Hall, E. Frank, G. Holmes, B. Pfahringer, P. Reutemann, I. H. Witten, The WEKA data mining software: An update. *ACM SIGKDD Explor. Newsl.* **11**, 10–18 (2009).
19. T. Sing, O. Sander, N. Beerenwinkel, T. Lengauer, ROCR: Visualizing classifier performance in R. *Bioinformatics* **21**, 3940–3941 (2005).
20. Team RDC, *R: A Language and Environment for Statistical Computing* (R Foundation for Statistical Computing, Vienna, 2009).

Acknowledgments: We would like to gratefully acknowledge the patients who consented to participate. **Funding:** This work was supported under the Clinical and Translational Science Awards NIH UL1 RR025774 and the American Reinvestment and Recovery Act funding ARRA UL1 RR025774-S1. A.H.C., J.J., C.R., and M.C. are employees of Veridex, LLC, Huntingdon Valley, PA 19006, USA. **Author contributions:** E.J.T. conceived and designed the study and obtained the funding. The following authors participated in the design and/or interpretation of the reported experiments or results. A.B., K.B., B.C., A.H.C., M.C., S.D., V.M.F., R. Gollapudi, R. Goldberg, S.H., J.J., S.K., P.K., O.L., C.R., N.J.S., E.J.T., S.T., and M.W. The acquisition and/or analysis of data was handled by A.B., A.H.C., M.C., S.D., V.M.F., R. Gollapudi, R. Goldberg, S.H., J.J., S.K., P.K., O.L., C.R., K.R., N.J.S., R.S., S.T., and M.W. Drafting and/or revising the manuscript for critical content was executed between A.B., K.B., B.C., A.H.C., M.C., S.D., V.M.F., S.H., J.J., S.K., P.K., O.L., C.R., K.R., N.J.S., E.J.T., and S.T. The following authors were primarily responsible for a particular, specialized role in the research: A.B., B.C., A.H.C., M.C., S.D., R. Gollapudi, R. Goldberg, P.K., O.L., K.R., N.J.S., R.S., E.J.T., S.T., and M.W. Administrative, technical, or supervisory tasks were handled by A.B., B.C., A.H.C., M.C., S.D., V.M.F., S.H., J.J., S.K., P.K., C.R., K.R., N.J.S., E.J.T., S.T., and M.W. **Competing interests:** E.J.T. is an author on a patent associated with this work: patent application number 61/505,481 (July 07, 2011), Method of Analyzing Cardiovascular Disorders and Uses Thereof.

Submitted 14 November 2011
Accepted 29 February 2012
Published 21 March 2012
10.1126/scitranslmed.3003451

Citation: S. Damani, A. Bacconi, O. Libiger, A. H. Chourasia, R. Serry, R. Gollapudi, R. Goldberg, K. Rapeport, S. Haaser, S. Topol, S. Knowlton, K. Bethel, P. Kuhn, M. Wood, B. Carragher, N. J. Schork, J. Jiang, C. Rao, M. Connelly, V. M. Fowler, E. J. Topol, Characterization of circulating endothelial cells in acute myocardial infarction. *Sci. Transl. Med.* **4**, 126ra33 (2012).

Downloaded from stm.sciencemag.org on March 21, 2012